Journal of
Medicinal Chemistry

Article

N-Aryl-3-mercaptosuccinimides as Antivirulence Agents Targeting Pseudomonas aeruginosa Elastase and Clostridium Collagenases

Jelena Konstantinovi#, Samir Yahiaoui, Alaa Alhayek, Jörg Haupenthal, Esther Schönauer, Anastasia Andreas, Andreas M Kany, Rolf Mueller, Jesko Köhnke, Fabian Berger, Markus Bischoff, Rolf W. Hartmann, Hans Brandstetter, and Anna K.H Hirsch

J. Med. Chem., **Just Accepted Manuscript** • Publication Date (Web): 29 May 2020

Just Accepted

is published by the American Chemical Society. 1155 Sixteenth Street N.W., Washington, DC 20036

N-Aryl-3-mercaptosuccinimides as Antivirulence Agents Targeting *Pseudomonas aeruginosa* Elastase and *Clostridium* Collagenases

Jelena Konstantinović[1,⊥], Samir Yahiaoui[1,⊥], Alaa Alhayek[1,2,⊥], Jörg Haupenthal[1], Esther Schönauer[3], Anastasia Andreas[4], Andreas M. Kany[1], Rolf Müller[2,4], Jesko Köhnke[5], Fabian K. Berger[6], Markus Bischoff[6], Rolf W. Hartmann[1,2], Hans Brandstetter[3], Anna K.H. Hirsch[1,2,]*

[1]Department of Drug Design and Optimization, Helmholtz Institute for Pharmaceutical Research Saarland (HIPS) – Helmholtz Centre for Infection Research (HZI), Campus Building E8.1, 66123 Saarbrücken, Germany

[2]Department of Pharmacy, Saarland University, Campus Building E8.1, 66123 Saarbrücken, Germany

[3]Department of Biosciences, University of Salzburg, Billrothstr. 11, 5020 Salzburg, Austria

[4]Department of Microbial Natural Products, Helmholtz Institute for Pharmaceutical Research Saarland (HIPS) – Helmholtz Centre for Infection Research (HZI), Campus Building E8.1, 66123 Saarbrücken, Germany

[5]Workgroup Structural Biology of Biosynthetic Enzymes, Helmholtz Institute for Pharmaceutical Research Saarland (HIPS), Campus Building E8.1, 66123, Saarbrücken, Germany

[6]Institute of Medical Microbiology and Hygiene, Saarland University, 66421 Homburg/Saar, Germany

Key words: virulence factor, LasB, ColH, metalloprotease inhibitor, succinimide, thiol, *Hathewaya histolytica*

ABSTRACT: In light of the global antimicrobial-resistance crisis, there is an urgent need for novel bacterial targets and antibiotics with novel modes of action. It has been shown that *Pseudomonas aeruginosa* elastase (LasB) and *Clostridium histolyticum* (*Hathewaya*

histolytica) collagenase (ColH) play a significant role in the infection process and thereby represent promising antivirulence targets. Here, we report novel *N*-aryl-3-mercaptosuccinimide inhibitors that target both LasB and ColH, displaying potent activities *in vitro* and high selectivity for the bacterial over human metalloproteases. Additionally, the inhibitors demonstrate no signs of cytotoxicity against selected human cell lines and in a zebrafish embryo toxicity model. Furthermore, the most active ColH inhibitor shows a significant reduction of collagen degradation in an *ex vivo* pig skin model.

▪ INTRODUCTION

The growing number of antibiotic-resistant bacteria represents one of the biggest risks to public health, leading to an enhancement of infections that are difficult to treat. Bacterial resistance to antibiotics is natural, yet overuse and misuse of antibiotics accelerate resistance development, bringing the world to the verge of the so-called “post-antibiotic era”. Of special importance are infections caused by multi-drug resistant bacteria on the WHO priority-pathogen list,[1] such as carbapenem-resistant variants of the Gram-negative

pathogen *Pseudomonas aeruginosa,*[2] which are responsible for many nosocomial,[3] eye and burn infections,[4,5] as well as fatal lung infections in cystic-fibrosis and bronchiectasis patients.[6,7] *P. aeruginosa* also affects injured tissue such as skin *via* surgical or wound infections.[8] The versatile pathogen is known to produce numerous virulence factors.[9] One of them is elastase, the metalloenzyme that shows hydrolytic activity towards connective tissue, which significantly contributes to the effectiveness of this bacteria.[10] Clostridiaceae represent a family of Gram-positive bacteria that are known as causative agents of numerous fatal diseases with high mortality rates worldwide, such as botulism (*Clostridium botulinum*), soft-tissue infections like gas gangrene and wound infections (*Clostridium perfringens*, *Clostridium histolyticum*) and tetanus (*Clostridium tetani*).[11,12] *Bacillus cereus* is another Gram-positive bacterium responsible for foodborne illnesses and traumatic wound infections in humans.[13,14] The high lethality of these bacteria is closely related to the production of collagenases, extracellular enzymes that enable the bacteria to colonize specific niches in the host, to evade the host immune response and to obtain nutrition from infected cells. Moreover, collagenases cause tissue destruction *via* collagen degradation, which plays a significant role in the infection process by allowing

the bacteria to reach anaerobic sites in host tissue and spread the infection.[15,16] This especially affects the wound-infection prognosis and results in delayed healing process.[17,18]

Recently, particular emphasis has been put on targeting bacterial virulence as an alternative approach for fighting microbial infections. The pursued 'pathoblockers' preserve the commensal microbiome and are expected to be less susceptible to the development of resistance than conventional antibiotics. In our work, we focus on two zinc metalloproteases that are secreted virulence factors: elastase (LasB) from *P. aeruginosa* and collagenase H (ColH) from *C. histolyticum* (recently renamed as *Hathewaya histolytica*[19]). Both enzymes have a major impact on the infectivity of *P. aeruginosa* and *C. histolyticum*.[11,20] Moreover, their extracellular localization makes these enzymes particularly attractive targets, considering the difficulties associated with crossing the Gram-negative bacterial cell walls in the former species.

Most of LasB and ColH inhibitors found in the literature contain different metal-chelating warheads.[20,21,22,23,24] Among them, hydroxamates represent the most common structural motif.[21,25,26,27] The main problem with such hydroxamate-containing protease inhibitors is

their lack of stability under physiological conditions and their lack of selectivity over human matrix metalloproteases (MMPs), which makes them unsuitable candidates for antibacterial treatment *in vivo*[26,28] and rationalizes why there is still no drug on the market that could effectively inhibit these virulence factors. A selection of LasB and ColH inhibitors described in the literature is shown in Figure 1.

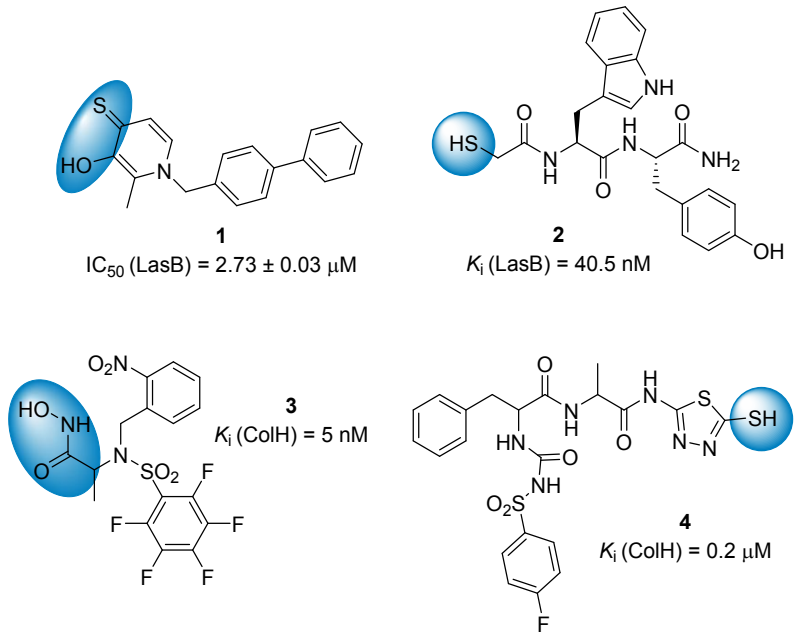

Figure 1. Structural motifs of some LasB and ColH inhibitors described in the literature (Zn-binding groups are highlighted in blue).[21,22,24,26]

In our previous work, we discovered *N*-aryl mercaptoacetamide inhibitors with low micromolar and nanomolar affinities toward LasB and ColH, respectively.[29,30] To constrain

the flexibility and freeze the active conformation of our previously published thiols, we designed a novel succinimide class (Figure 2). The succinimide core has been reported for inhibitors of various enzyme targets, such as serine proteases,[31] human leukocyte elastase, cathepsin G and proteinase 3,[32] tumor necrosis factor and phosphodiesterase.[33] It can also be found in several drugs, such as ethosuximide, phensuximide, methsuximide and lurasidone, used to treat absence seizures, schizophrenia and bipolar disorder.[34]

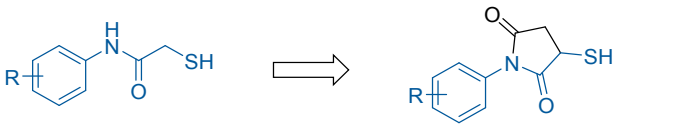

N-aryl mercaptoacetamides 3-mercapto-*N*-arylsuccinimides

5: R= 3,4-di-Cl **(IC_{50} (LasB) = 6.6 ± 0.3 µM)**
6: R= 4-Ac **(IC_{50} (ColH) = 0.017 ± 0.002 µM)**

Figure 2. Our previous results and the design of new inhibitors.[29,30]

Here, we report new *N*-aryl-3-mercaptosuccinimides, showing low micromolar potencies against *P. aeruginosa* elastase and nanomolar potencies against *Clostridium* collagenases. The most active compounds were investigated for their cytotoxicity and selectivity for the bacterial over human metalloproteases. To validate collagenases as targets, we have established an *ex vivo* pig skin model and demonstrated the impact of our most potent inhibitor on this human skin mimic.

▪ RESULTS AND DISCUSSION

Design of new compounds. We designed the initial succinimide core based on our previously published *N*-aryl mercaptoacetamide inhibitors.[29,30] To expand the structure–activity relationships (SAR) further and provide more detailed information on the aromatic moiety's influence on the activity, we designed a series of compounds bearing polar, lipophilic, electron-withdrawing or electron-donating functional groups. In order to prevent disulfide formation, we protected the free thiol group in the form of thioacetate. Finally, we explored the possibility of growing the structure further by introducing an additional carbon spacer between the succinimide and the free thiol.

Synthesis of new compounds. Reaction of anilines with mercaptosuccinic acid at 120–160 °C afforded 21 new free thiol-containing succinimides **7–27** with yields of 6–68%. Due to the presence of an *ortho*-substituent, compounds **16–18** and **21** were obtained as mixtures of atropisomers. Acetic anhydride in presence of pyridine and DMAP at room temperature led to protection of the free thiol group to obtain derivatives **28–30** with moderate yields (65–78%). The general synthetic route is presented in Scheme 1.

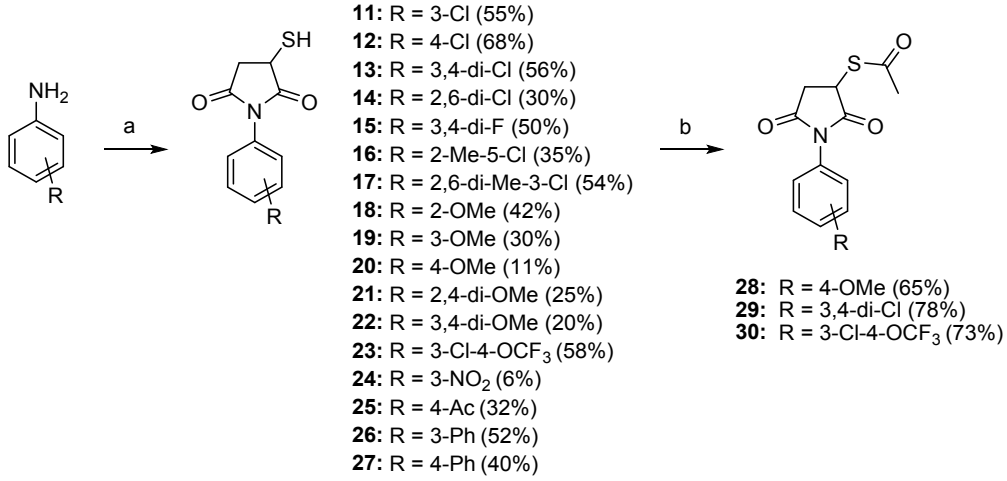

Scheme 1. Synthesis of novel free thiol succinimides and thioacetate derivatives

Synthesis of *N*-aryl-3-mercaptomethylsuccinimides started from itaconic anhydride and corresponding anilines (Scheme 2). Cyclization of intermediate α-itaconamic acids **31**, **32**, **34** and **35** in presence of acetic anhydride and sodium acetate at 100 °C,[35] afforded itaconimides **36–39** with relatively low yields (8–39%). Michael addition of thioacetic acid on obtained itaconimides in presence of triethylamine in dimethoxyethane at room temperature, led to the final compounds **40–43** with high yields (61–99%). α-Itaconamic acids **32–34** under the same reaction conditions in THF as a solvent, provided compounds **44–46** with quantitative yields. Hydrolysis of thioacetate using sodium

hydroxide in methanol at room temperature afforded free thiol-containing carboxylic acids **47–49** with moderate to quantitative yields (61–99%). A final neat cyclization step furnished target compounds **50–52** with low yields (14–36%).

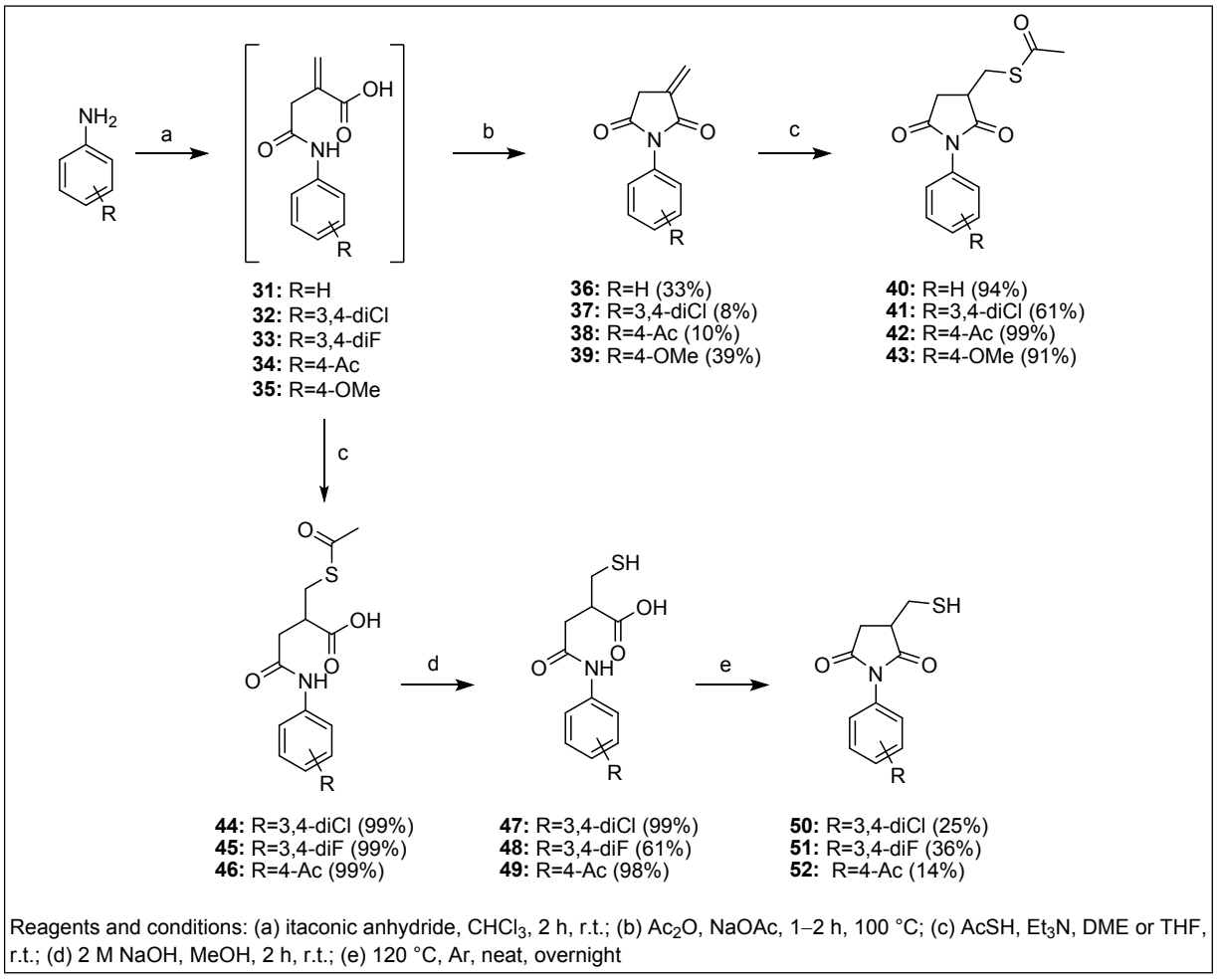

Scheme 2. Synthesis of *N*-aryl-3-mercaptomethylsuccinimides and their acetylthio analogues

Activity against antivirulence targets. We evaluated all compounds synthesized in this work for their inhibitory activity against both LasB and ColH. IC_{50} values and percentage of inhibition results were calculated from at least two independent experiments performed in duplicates.

SAR of novel succinimides on LasB. To expand the SAR, we designed and synthesized 31 succinimide-based derivatives and investigated their inhibitory activity against LasB using a functional FRET-based *in vitro* assay (Table 1).[36] Among the first group of compounds **7**–**27**, electronegative substituents such as chlorine or fluorine were found to be favorable for the activity. In particular, compounds **13** and **15**, both with a 3,4-dihalo pattern, displayed more potent inhibitory activities when compared to the *ortho*-, *meta*- or *para*-monosubstituted analogues. Furthermore, several examples indicate that polar groups, particularly electron-donating substituents are detrimental for the activity. In fact, all mono and dimethoxy derivatives were less potent than their chlorine analogues, with 3,4-dimethoxy derivative **22** showing the most dramatic loss in activity (47-fold compared to **13**). This is further supported by the five-fold difference in activity between 3,4-dimethyl (**9**) and 3,4-dimethoxy analogues (**22**). Among both chlorine and methoxy isomers, *ortho*-

(**10** and **18**) and *meta*-derivatives (**11** and **19)** proved to be more potent than the *para*-derivatives (**12** and **20**), most probably due to electronic effects or disruptions of the planar structure caused by the vicinity of the substituents to the succinimide core. Compound **25** with its polar electron-withdrawing *para*-acetyl substituent was 1.7 times more active than its methoxy-analogue, but still much less potent than compounds bearing lipophilic chlorine substituents. The observation that polar, electron-withdrawing substituents are more tolerated than electron-donating ones, is illustrated through the example of nitro-compound **24**, being more active than its 3-methoxy analogue **19**. Compounds with an additional phenyl ring in positions 3 (**26**) and 4 (**27**) showed comparable activity to the compound with a naked core, with 3-phenyl derivative even being 1.6–fold more active than compound **7**. Although these derivatives were less potent than compound **13**, the fact that they show inhibition of LasB paves the way for further optimization of this part of the structure. In addition, the fact that compounds **8** (R^1=4-Me) and **27** (R^1=4-Ph) show no significant difference in the activity suggests that there are no steric limitations in *para*-position. An additional carbon spacer next to the free thiol in compounds **50** and **51** did not improve the activities of the most potent derivatives **13** and **15**, respectively. However,

the IC_{50} values determined for **50** and **51**, being in the range of 5–10 μM, open the possibility to further grow the structure in the direction of the free thiol group. All thioacetate derivatives, with no exception, proved to be inactive, with <50% of inhibition at 200 μM, which confirms that the free thiol is crucial for the activity against LasB.

Table 1. Structures and LasB inhibition of a series of novel succinimide derivatives: 3,4-di-halo pattern in **13**, **15** and **50** proved to be beneficial for the activity.[a]

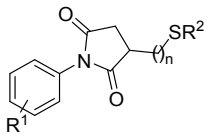

Cpd.	R^1	R^2	n	IC_{50} (μM)	Cpd.	R^1	R^2	n	IC_{50} (μM)
7	H	H	0	44.2±2.3	**23**	3-Cl-4-OCF_3	H	0	55.2±4.4
8	4-Me	H	0	50.6±1.6	**24**	3-NO_2	H	0	22.2±0.4
9	3,4-di-Me	H	0	29.4±0.9	**25**	4-Ac	H	0	64.0±7.5
10	2-Cl	H	0	8.5±0.4	**26**	3-Ph	H	0	27.6±4.0
11	3-Cl	H	0	8.1±0.5	**27**	4-Ph	H	0	44.6±1.1
12	4-Cl	H	0	16.5±0.8	**28**	4-OMe	Ac	0	>200
13	3,4-di-Cl	H	0	**3.4±0.2**	**29**	3,4-di-Cl	Ac	0	>200
14	2,6-di-Cl	H	0	16.0±3.7	**30**	3-Cl-4-OCF_3	Ac	0	>200

15	3,4-di-F	H	0	**3.5±0.2**	**40**	H	Ac	1	>200
16	2-Me-5-Cl	H	0	15.0±0.6	**41**	3,4-di-Cl	Ac	1	>200
17	2,6-di-Me-3-Cl	H	0	30.5±5.4	**42**	4-Ac	Ac	1	>200
18	2-OMe	H	0	28.9±1.6	**43**	4-OMe	Ac	1	>200
19	3-OMe	H	0	40.2±1.4	**50**	3,4-di-Cl	H	1	**5.4±0.7**
20	4-OMe	H	0	111.8±8.9	**51**	3,4-di-F	H	1	10.1±1.4
21	2,4-di-OMe	H	0	45.0±0.8	**52**	4-Ac	H	1	>200
22	3,4-di-OMe	H	0	160.2±10.1					

[a]Means and SD of at least two independent experiments.

SAR of novel succinimides on ColH. In our previous work, we have shown that there is a structural similarity between the inhibitors of LasB and ColH.[29,30] It was therefore of interest to investigate the activity of all new compounds against ColH and to compare the SAR with that observed for LasB. Figure 3 represents the inhibition of the peptidase domain of ColH (ColH-PD) in the presence of 1 µM of the selected compounds. Previously, we reported that polar substituents in *para*-position have the most beneficial effect on the activity of *N*-aryl mercaptoacetamides.[30] Here, we observed the same trend with the new succinimide class, with compound **25**, bearing a *para*-acetyl substituent, being the most active one with 95% of ColH-PD inhibition. The *para*-methoxy derivative

20 was slightly less active with 74% of inhibition, but still following the trend of polar substituents being more favorable for the activity than non-polar, lipophilic substituents, such as chlorine. The protection of the free thiol functional group proved to be detrimental for the activity, as in the case of LasB. The two compounds showing >50% of inhibition of ColH-PD were further tested in a dose-response manner in the presence of the reducing agent TCEP. This experiment revealed nanomolar IC_{50} values for **25** (0.06 ± 0.01 μM) and **20** (0.32 ± 0.05 μM). Overall, since the inhibitors presented in this work have similar structure and SAR we described for *N*-aryl mercaptoacetamides, we expect the interactions with LasB and ColH to be similar as those in our previously published co-crystal structures.[29,30]

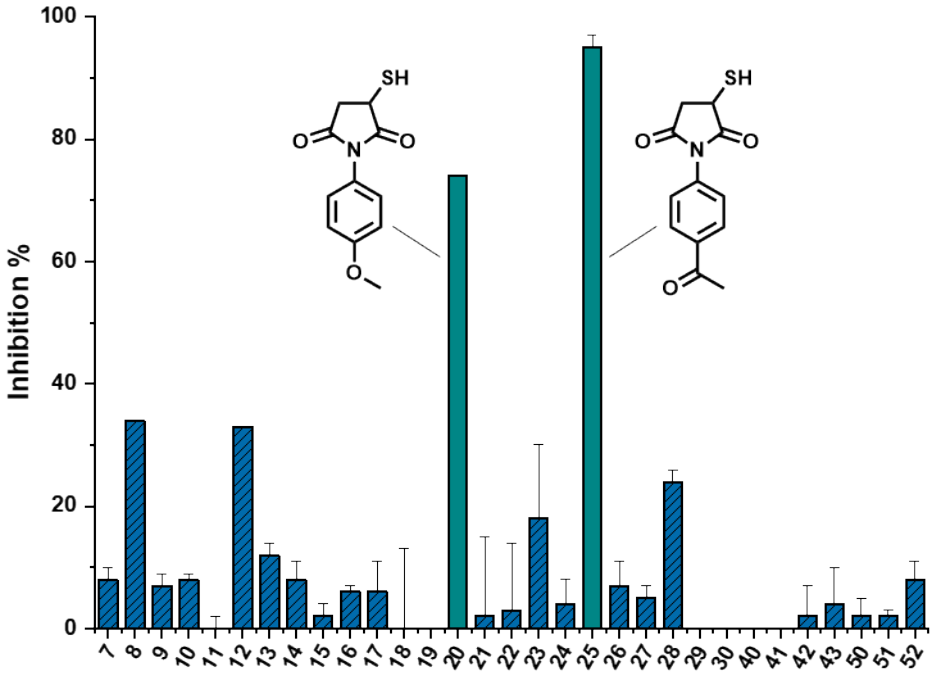

Figure 3. Inhibition of the peptidolytic activity of ColH-PD in the presence of 1 μM of the respective compound in a FRET-based assay: *para*-acetyl substituent in compound **25** proved to be the most beneficial substitution for the activity. Data are presented as means and SD of three independent experiments.

We consider the difference observed in SARs between LasB and ColH inhibitors beneficial in terms of their selectivity for each particular target. Each hit can be further developed for the treatment of single infections caused by either *P. aeruginosa* or *C.*

histolyticum. However, wound infections, due to their nature, are likely to be colonized with other bacteria.[37,38] Therefore, having a common structural motif that inhibits both targets is particularly interesting and if the inhibitors were to be used for Clostridia and *P. aeruginosa* co-infections purpose, their structure could be further optimized and adapted as dual inhibitors of ColH and LasB.

Broad-spectrum inhibition of other bacterial collagenases. In addition to ColH from *C. histolyticum*, other *Clostridium* and *Bacillus* species also secrete collagenases that play pivotal roles in the pathogenesis of these bacteria by destroying the connective tissue components in the infected host.[16] We therefore tested the two most active ColH-PD inhibitors (**20** and **25**) on three additional collagenases, using the collagenase unit of ColG (ColG-CU) from *C. histolyticum*, the peptidase domain of ColT (ColT-PD) from *C. tetani*, and the collagenase unit of ColQ1 (ColQ1-CU) from *B. cereus* strain Q1. As anticipated, the succinimide-based scaffold retained the broad-spectrum inhibitory properties of the mercaptoacetamide-based inhibitors (Table 2).[30]

Table 2. Inhibition of ColH-PD, ColT-PD, ColG-CU and ColQ1-CU in presence of 100 μM of compounds **20** and **25**[a]

	% inhibition @ 100 μM			
Cpd.	**ColH-PD**	**ColG-CU**	**ColT-PD**	**ColQ1-CU**
20	95 ± 1	85 ± 3	89 ± 4	99 ± 1
25	96 ± 2	100 ± 2	102 ± 3	99 ± 2

[a]Means and SD of at least two independent experiments.

Selectivity against MMPs, HDACs and TACE as human off-targets. Previously, we described *N*-aryl mercaptoacetamides with high selectivity for the bacterial over a broad range of human MMPs.[29,30] MMPs are calcium-dependent zinc metalloproteases that play a pivotal role in numerous biochemical processes in humans.[39,40] Based on the depth of their S1' binding pocket, MMPs can be divided into three classes: deep (*e.g.*, MMP-3 and -14), intermediate (*e.g.*, MMP-2 and -8) and shallow (*e.g.*, MMP-1 and -7). With the aim to explore the interactions of our inhibitors with all three pocket types, which could help us to assess potential effects on other, not-tested representatives, we chose a panel of six MMPs, comprising two members of each class. In addition, HDAC-3, HDAC-8 and

TACE (ADAM-17) – enzymes involved in gene expression and the processing of TNF-α[41,42] respectively – were selected as important additional human off-targets. Our results showed that the most potent inhibitors of LasB and ColH (**13** and **25**, respectively) fortunately possess a high selectivity over most of the off-targets tested. While both compounds did not inhibit MMPs -1, -3 and -7 as well as both HDAC enzymes, we observed certain inhibition of MMP-2, -8 and -14 at 100 µM. Inhibition of TACE, which was observed for both compounds, will be considered as high priority in the future optimization of the structures (Tables 3 and 4).

Table 3. Inhibition of six MMPs in presence of 100 µM of compounds **13** and **25**[a]

	% inhibition @ 100 µM					
Cpd.	**MMP-1**	**MMP-2**	**MMP-3**	**MMP-7**	**MMP-8**	**MMP-14**
13	n.i.	39 ± 32	n.i.	n.i.	84 ± 8	n.i.
25	n.i.	14 ± 4	n.i.	n.i.	94 ± 1	84 ± 8

[a]Means and SD of at least two independent experiments. n.i. = <10% inhibition.

Table 4. Activity of compounds **13** and **25** against HDAC-3, HDAC-8 and TACE[a]

	IC_{50} (μM)		
Cpd.	HDAC-3	HDAC-8	TACE
13	>100	>100	5.2 ± 0.6
25	>100	>100	3.4 ± 1.2

[a]Means and SD of at least two independent experiments.

Cytotoxicity assays. Broad-spectrum inhibition of bacterial collagenases and selectivity against a panel of off-targets supported the further evaluation of the compounds' toxicity *in vitro*. In this context, we investigated **13** and **25**, the two most active compounds against both targets, for their cytotoxicity against the three human cell lines – HepG2 (hepatocellular carcinoma), HEK293 (embryonal kidney) and A549 (lung carcinoma). Neither compounds showed cytotoxic effects, with IC_{50} values > 100 μM (Table 5), making them suitable for further investigation in *in vivo* model systems. Compared to our previous hits, **5** and **6**, they displayed similar or even lower toxicities in most of the cell lines tested. Particularly, compound **25** proved to be even less toxic than **6**, which showed an IC_{50} of 100 μM in HEK293 cells.

Table 5. Cytotoxicity of compounds **13**, **25**, **5** and **6** against HepG2, HEK293 and A549 cell lines[a]

	IC_{50} (μM)		
Cpd.	**HepG2**	**HEK293**	**A549**
13	>100	>100	>100
25	>100	>100	>100
5	>100	>100	>100
6	>100	100	>100

[a]Means and SD of at least two independent experiments

***In vivo* toxicity in zebrafish embryo model.** Due to the promising *in vitro* activities against antivirulence targets LasB and ColH, and the lack of cytotoxicity against three human cell lines, we subjected compounds **15** and **25** to a toxicity study based on zebrafish embryos. An advantage of this non-mammalian *in vivo* model is the high genetic homology to humans and that it provides follow-up information on the type of toxicity encountered (*e.g.*, hepatic, cardio-vascular *etc.*). In addition, this model can also predict mammalian teratogenicity by evaluation of lethality and malformation during the development of

embryonic zebrafish.[43,44] Both compounds tested showed a maximum tolerated concentration (MTC) of ≥ 30 µM, which is higher than for the corresponding mercaptoacetamide-based LasB inhibitor **5** we published previously (MTC = 10 µM) (Table S1).[29]

***Ex vivo* pig skin model.** We established an *ex vivo* model based on pig skin to address the impact of our inhibitors on living mammalian tissue and on the contained collagen as the natural substrate of collagenase. We challenged the skin, prepared from the ear of freshly slaughtered pigs, with pure ColQ1 from *B. cereus* to degrade collagen. We assessed the activity of ColQ1 by quantifying the formation of hydroxyproline as an indicator for collagen turnover (Figure 4). Optimization of the assay conditions for the model consisted of examining different buffer conditions and different protein concentrations (Figure S1 and Figure S2). To evaluate the potential effect of **25** on collagen turnover, we incubated the skin with ColQ1 in absence and presence of defined concentrations of this compound. The subsequent quantification of hydroxyproline revealed that **25** inhibited the collagenolytic activity of ColQ1, as demonstrated by the significantly reduced amount of hydroxyproline released compared to control (Figure 5).

These results support our previous finding that **25** is an inhibitor of a broad range of bacterial collagenases. The good performance of our inhibitors in this model is a sound starting point for their subsequent testing under *in vivo* conditions. We expect that our inhibitors will accelerate the *in vivo* healing process, by preventing the distribution of infection. The immune system will clear the bacteria, promoting remodeling of collagen and skin regeneration.

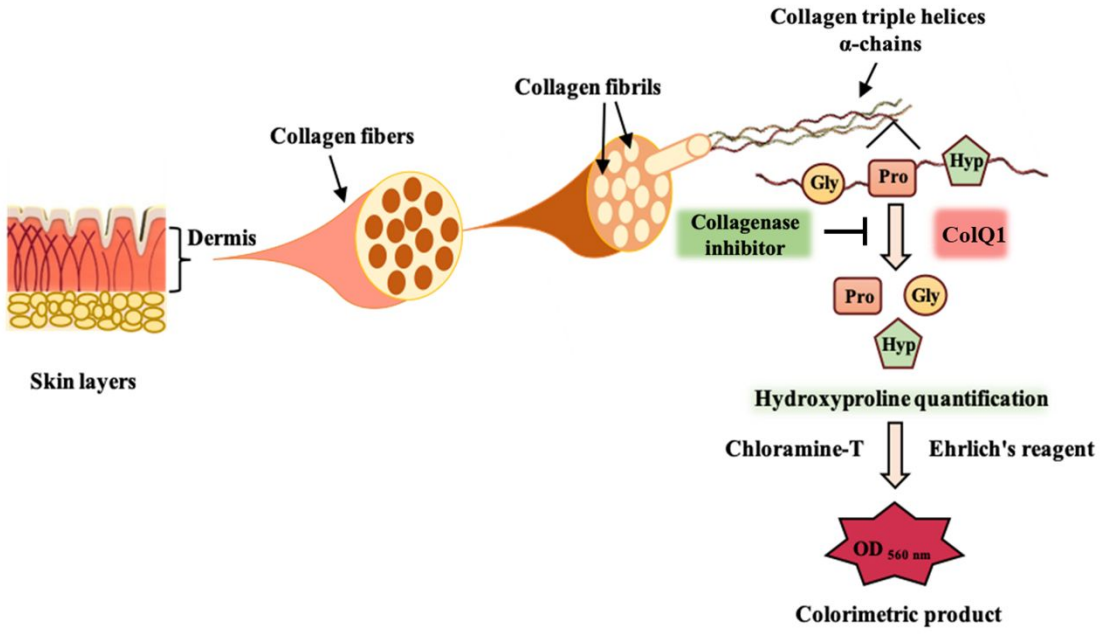

Figure 4. Representation of the pig skin model: the composition of the skin, the dermal layer and the amino acids of collagen are illustrated. The concept of the hydroxyproline

quantification assay is explained by mixing chloramine-T and Ehrlich's reagent to obtain a product that can be detected with a spectrophotometer.

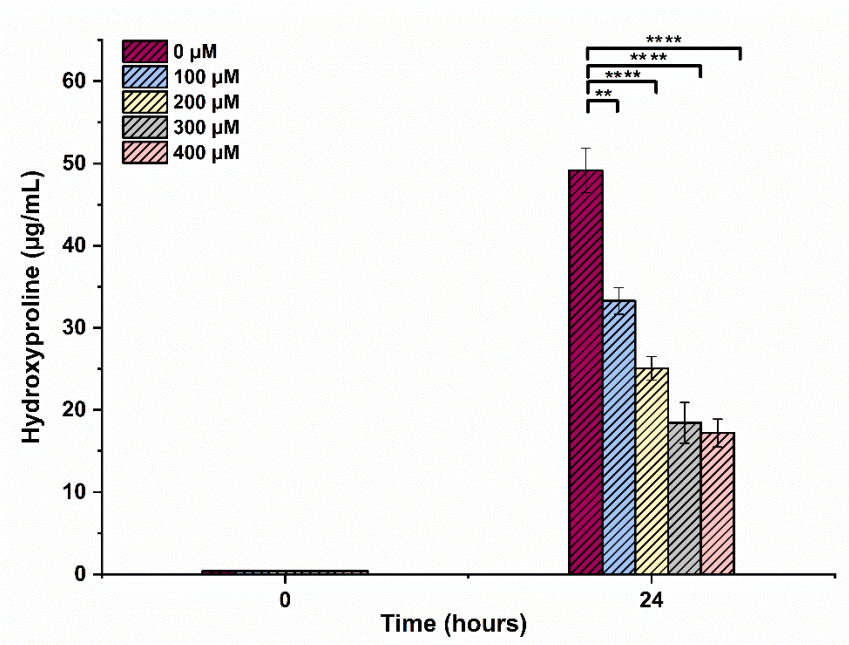

Figure 5. The amount of hydroxyproline at different concentrations of **25**. Data shown represent the means ± SD from three independent measurements. One-way ANOVA followed by Tukey's HSD test (** = p < 0.01, **** = $p < 0.0001$).

Antibacterial activity. The aim of this study was to create 'pathoblockers' that target bacterial virulence factors without directly affecting bacterial viability. These have the

ability to disarm, rather than to kill pathogens in order to make them less pathogenic. In this context, it was of interest to test the antibacterial activity of the new derivatives against *P. aeruginosa* strain PA14 and *C. histolyticum* strain DSM 1126 to exclude growth inhibition by selected compounds. We therefore selected the four most potent compounds against LasB (**13**, **15**, **50** and **51**) and the most active succinimide against ColH (**25**). As shown in Table 6, it is clear that compounds **13**, **15**, **50** and **51** did not affect the growth of PA14 and **25** did not affect the growth of DSM 1126, with a minimal inhibitory concentration (MIC) > 100 μM. This assures that the activity of these compounds is only through targeting the secreted bacterial virulence factors.

Table 6. Antibacterial activity of selected compounds against *P. aeruginosa* and *C. histolyticum*

	MIC (μM)	
Cpd.	*P. aeruginosa*	*C. histolyticum*
13	>100	n.d.
15	>100	n.d.
50	>100	n.d.

51	>100	n.d.
25	n.d.	>100

n.d. = not determined

▪ CONCLUSIONS

In this study, we aimed to constrain the conformation of previously published *N*-aryl mercaptoacetamide inhibitors,[29,30] which led to a series of novel succinimide inhibitors of the antivirulence targets LasB and ColH. Among these compounds, we identified **13** and **25** to show the best potency against LasB and ColH, respectively. Compound **13** improved the activity against LasB compared to our previous hit **5** by two times, while compound **25** was slightly less potent than **6** against ColH; however, it maintained the activity in the nanomolar range. Both compounds showed sufficient selectivity for the bacterial metalloproteases over human MMPs and three other off-targets. The two most active compounds against ColH, **25** and **20**, showed in addition broad-spectrum inhibition of homologous bacterial collagenases. These most potent LasB and ColH inhibitors showed no signs of cytotoxicity in three human cell lines. Interestingly, compounds **15** and **25** showed a MTC of ≥ 30 μM in our zebrafish model. This is, for **15,** a threefold lower

toxicity compared to our published LasB hit **5**. Moreover, we have established a pig skin model to further characterize the most promising collagenase inhibitor. In this *ex vivo* assay, compound **25** showed a promising effect in preventing collagen degradation, which paves the way for this compound's further evaluation under *in vivo* conditions. To investigate the compounds in such *in vivo* models, additional work should be carried out to improve their pharmacokinetic profiles. However, we strongly believe that the new succinimide inhibitors presented in this work have a great potential to be developed further and to be used as therapeutics.

▪ EXPERIMENTAL SECTION

Chemistry. All reagents were used from commercial suppliers without further purification. Procedures were not optimized regarding yield. NMR spectra were recorded on a Bruker AV 500 (500 MHz) spectrometer. Chemical shifts are given in parts per million (ppm) and referenced against the residual proton, ^{1}H, or carbon, ^{13}C, resonances of the >99% deuterated solvents as internal reference. Coupling constants (J) are given in Hertz. Data are reported as follows: chemical shift, multiplicity (s = singlet, d = doublet, t

= triplet, q = quartet, m = multiplet, dd = doublet of doublets, dt = doublet of triplets, br = broad and combinations of these) coupling constants, and integration. Liquid chromatography-mass spectrometry was performed on a LC-MS system, consisting of a Dionex UltiMate 3000 pump, autosampler, column compartment and detector (Thermo Fisher Scientific, Dreieich, Germany) and ESI quadrupole MS (MSQ Plus or ISQ EC, Thermo Fisher Scientific, Dreieich, Germany). High resolution mass was determined by LC-MS/MS using Thermo Scientific Q Exactive Focus Orbitrap LC-MS/MS system. Purity of the final compounds was determined by LC-MS using the area percentage method on the UV trace recorded at a wavelength of 254 nm and found to be >95%. Melting points were determined by using a Stuart melting point SMP30 device.

General procedure A: Synthesis of succinimides 7–27 and 50–52

Mercaptosuccinic acid (1.0 eq) and corresponding aniline (1.0 eq) were mixed in a crimp vial under Ar atmosphere and heated at 120–160 °C from 3.5 h to overnight. The crude product was purified using column chromatography. In case of *N*-aryl-3-

mercaptomethylsuccinimides, 4-(aminoaryl)-2-(mercaptomethyl)-4-oxobutanoic acid was heated at 120 °C overnight.

General procedure B: Synthesis of thioacetates 28–30 by acetylation of free thiol

Succinimide (1.0 eq) was dissolved in DCM and the solution was cooled in an ice bath. Pyridine (2.0 eq) and DMAP (0.1 eq) were added, followed by dropwise addition of Ac_2O (2.0 eq). After 30 minutes at 0 °C, the reaction mixture was allowed to warm up to r.t. and stirred overnight. Volatiles were evaporated under reduced pressure and crude product was purified using column chromatography.

General procedure C: Synthesis of a-itaconamic acids 31–35

α-Itaconamic acids were synthesized following the procedure described in the literature.[35] Itaconic anhydride (1.0 eq) was dissolved in $CHCl_3$. The corresponding aniline (1.0 eq) was added to the vigorously stirring solution. After 2 h, the product was collected by filtration and washed with small amount of chloroform. The product was used in the next step without further purification.

General procedure D: Synthesis of itaconimides 36–39

Itaconimides were synthesized following the procedure described in the literature from intermediate α-itaconamic acids described in general procedure C.[35] α-Itaconamic acid (1.0 eq) was mixed with NaOAc (0.5 eq) and Ac_2O (3.5 eq) and heated at 100 °C for 1–2 h. The dark reaction mixture was cooled to r.t., poured into the ice-cold water and extracted 3 times with EtOAc. Combined organic layers were washed with brine and dried over anh. Na_2SO_4. Crude product was purified using column chromatography. In all cases except in the case of 4-OMe derivative, the corresponding citraconimides were isolated as a side product and therefore the yield of obtained itaconimides was low to moderate.

General procedure E: Synthesis of thioacetates 40–46 using Michael addition

Corresponding itaconimide/α-itaconamic acid (1.0 eq) was dissolved in DME/DCM/THF under Ar atmosphere. Thioacetic acid (1.1–1.5 eq) was added, followed by Et_3N (0.01–0.1 eq). The reaction mixture was stirred at r.t. overnight. Crude product was purified using column chromatography or used in the next step without further purification.

General procedure F: Thioacetate hydrolysis to obtain compounds 47–49

Thioacetate (1.0 eq) was dissolved in methanol under Ar atmosphere and 2 M aqueous solution of NaOH (2.0–3.0 eq) was added. The reaction was stirred 1–2 h at r.t. After

quenching with 1M HCl, the reaction was extracted 3 times with EtOAc. Combined organic extracts were washed with brine and dried over anh. Na_2SO_4. The solvent was removed under reduced pressure. Crude product was purified using column chromatography or used in the next step without further purification.

1-(3,4-dichlorophenyl)-3-mercaptopyrrolidine-2,5-dione (13). Compound **13** was synthesized according to the general procedure A, using 3,4-dichloroaniline (162 mg, 1 mmol) and mercaptosuccinic acid (150 mg, 1 mmol), at 120 °C overnight. The product was purified using column chromatography (100% DCM). Final product was obtained as white solid (155 mg, 56%, M.p. 141 °C). ^{1}H NMR (500 MHz, DMSO-d6) δ ppm: 7.81 (d, *J* = 8.5 Hz, 1H), 7.62 (d, *J* = 2.0 Hz, 1H), 7.34 (dd, *J* = 2.0 , 8.5 Hz, 1H), 4.10 (dd, *J* = 4.5, 9.0 Hz, 1H), 3.87 (s, 1H), 3.37 (dd, *J* = 9.0, 18.0 Hz, 1H), 2.73 (dd, *J* = 4.5, 18.5 Hz, 1H). ^{13}C NMR (126 MHz, DMSO-d6) δ ppm: 176.2, 173.8, 132.4, 131.2, 131.1, 131.0, 128.9, 127.5, 39.2, 34.9. HRMS (ESI$^-$) m/z calcd. for $C_{10}H_6Cl_2NO_2S$ $[M-H]^-$ 273.94963, found 273.94931.

1-(4-acetylphenyl)-3-mercaptopyrrolidine-2,5-dione (25). Compound **25** was synthesized according to the general procedure A, using 4-aminoacetophenone (200 mg,

1.48 mmol) and mercaptosuccinic acid (222 mg, 1.48 mmol), at 120 °C overnight. The product was purified using column chromatography (Hex/EtOAc=7/3). Final product was obtained as pale yellow solid (117.1 mg, 32%, M.p. 104 °C). ^{1}H NMR (500 MHz, $CDCl_3$) δ ppm: 8.11–8.04 (m, 2H), 7.50–7.44 (m, 2H), 4.14–4.08 (m, 1H), 3.38 (dd, 1H, *J* = 9.3, 18.8 Hz), 2.77 (dd, 1H, *J* = 4.3, 18.8 Hz), 2.73 (d, 1H, *J* = 4.4 Hz), 2.63 (s, 3H). ^{13}C NMR (126 MHz, $CDCl_3$) δ ppm: 196.9, 175.6, 172.7, 136.9, 135.5, 129.2, 126.2, 37.4, 34.2, 26.7. HRMS (ESI^-) *m/z* calcd. for $C_{12}H_{10}NO_3S$ $[M-H]^-$ 248.038687, found 248.03867.

Expression and purification of LasB and ColH-PD. LasB and ColH-PD were expressed and purified as described previously.[29,45]

***In vitro* inhibition assays (LasB, ColH, ColT, ColG, ColQ1, MMPs, TACE, HDACs).** All *in vitro* inhibition assays were performed as described previously.[29,30] TACE and HDAC inhibitor screening kits were purchased from Sigma-Aldrich (Saint Louis, MO). The assays were performed according to the guidelines of the manufacturer. Fluorescence signals were measured using a CLARIOstar plate reader (BMG Labtech, Ortenberg, Germany).

Cytotoxicity assays. Cytotoxicity assays on HepG2, HEK293 and A549 cells were performed as described previously.[46]

Zebrafish embryo toxicity. Toxicity testing was performed according to the procedure described in the literature[47] with minor modifications using zebrafish embryos of the AB wild-type line at 1 day post fertilization (dpf). Embryos were collected and kept in a Petri dish at 28 °C until the next day in 0.3x Danieau's medium (17 mM NaCl, 2 mM KCl, 1.8 mM $Ca(NO_3)_2$, 1.5 mM HEPES (pH 7.1 – 7.3), 0.12 mM $MgSO_4$ and 1.2 µM methylene blue). The toxicity assay was performed using a 96-well plate with one embryo per well and 10 embryos per condition. To obtain compound concentrations between 2 µM and 100 µM, solutions of **15** and **25** were prepared freshly using 0.3x Danieau's medium with a final DMSO concentration of 1% (v/v). Single zebrafish embryos were placed in wells and directly incubated in the corresponding compound solutions. Monitoring of developmental defects, heart rate, touch-evoked locomotion response and survival rate was done daily (up to 120 hpf) via microscopy (Table S1). All of the described experiments were performed with zebrafish embryos < 120 hours post fertilization (hpf) and are not classified as animal experiments according to EU Directive 2010/63/EU. Protocols for

husbandry and care of adult animals are in accordance with the German Animal Welfare Act (§11 Abs. 1 TierSchG).

***Ex vivo* pig skin model.** Skin explants were obtained from pig ears, which were supplied by a local slaughterhouse. The explants were made using sterile medical biopsy punches (pfm medical, Cologne, Germany) with a diameter of 5 mm. The skin was washed once each with 70% isopropanol and sterile water, and three times with Dulbecco's Modified Eagle medium (DMEM) (Thermo Fisher Scientific, Schwerte, Germany) containing 1% penicillin and streptomycin. The punches were stored in DMEM medium and 15% glycerol at –80 °C until the time of the experiment. To do the experiment, a mixture of 300 nM of ColQ1, 4 mM $CaCl_2$, 10 µM $ZnCl_2$ and DMEM medium was prepared. The compound was preincubated with the mixture for 1 h at 37 °C and 5% CO_2. Afterwards, one skin explant was added to each well in a 24-well plate and incubated in an incubator at 37 °C and 5% CO_2 while shaking at 300 rpm. Aliquots of DMEM medium were taken at different time points in order to measure the formed hydroxyproline using a hydroxyproline assay kit (Sigma-Aldrich). This assay was performed according to the protocol of the manufacturer. Absorbance was measured using a PHERAstar plate reader (BMG Labtech). The

absorbance values were converted into the hydroxyproline concentration (µg/mL) using the calibration curve of hydroxyproline as a reference (Figure S3).

Bacterial growth inhibition assay. Assays regarding the determination of the MIC were performed as described recently for *P. aeruginosa* PA14.[48] MICs concerning *C. histolyticum* (*Hathewaya histolytica* (Weinberg and Séguin 1916) Lawson and Rainey 2016) DSM 1126 strain were performed in Brain Heart Infusion (BHI) medium. The Mc Farland standard was adjusted to 2 and followed by pre-dilution of 1:100. The dilution series of the substances (100 µM, 50 µM, 25 µM, 12.5 µM, 6.75 µM, 3.13 µM final concentration) was carried out in a 96-well plate in BHI and mixed with the bacterial suspension. The plates were subsequently incubated for 48 h at 37 °C under anaerobic conditions, followed by growth control and evaluation of MIC values. Given MIC values are means of at least two independent determinations.

Screening of the compounds for PAINS and prediction of BBB penetration. All the compounds that were tested in biological assays were screened for PAINS and possibility of BBB penetration using StarDrop software, Optibrium Ltd., Cambridge, UK (Table S2).

▪ AUTHOR INFORMATION

Corresponding authors

*anna.hirsch@helmholtz-hips.de

Author Contributions

⊥ J.K., S.Y. and A.A. contributed equally.

Funding Sources

A.K.H. Hirsch gratefully acknowledges funding from the European Research Council (ERC starting grant 757913) and the Helmholtz-Association's Initiative and Networking Fund. E. Schönauer thankfully acknowledges support by the Austrian Science Fund (FWF): P31843. J. Konstantinović acknowledges funding by the Alexander von Humboldt Foundation.

Notes

The authors declare no competing financial interest.

▪ ACKNOWLEDGMENTS

The authors thank J. Jung, D. Jener, A. Nimmesgern and M. Wiesbauer for excellent technical support and to A. Sikandar for providing purified LasB. The authors are furthermore grateful to the E. Färber GmbH & Co. KG for providing fresh pig ears and to R. Christmann for help regarding the pig skin assays.

▪ ABBREVIATIONS

LasB, *Pseudomonas aeruginosa* elastase; ColH, *Clostridium histolyticum* (*Hathewaya histolytica*) collagenase; MMPs, human matrix metalloproteases; SAR, structure–activity relationships; DMAP, 4-dimethylaminopyridine; Pyr, pyridine; DCM, dichloromethane; DME, dimethoxyethane; THF, tetrahydrofurane; IC_{50}, the half maximal inhibitory concentration; TCEP, Tris(2-carboxyethyl)phosphine hydrochloride; ColG-CU, collagenase unit of ColG from *C. histolyticum*; ColT-PD, the peptidase domain of ColT from *C. tetani*, ColQ1-CU, the collagenase unit of ColQ1 from *B. cereus* strain Q1; HepG2, hepatocellular carcinoma cell line; HEK293, embryonal kidney cell line; A549, lung carcinoma cell line; HDAC, histone deacetylase; TACE, tumor necrosis factor-α-

converting enzyme; MTC, maximum tolerated concentration; MIC, minimum inhibitory concentration; DMEM, Dulbecco's Modified Eagle's Medium.

▪ ASSOCIATED CONTENT

Supporting Information.

The following files are available free of charge.

Results of zebrafish embryo toxicity for compounds **15**, **25**, **5** and **6**, additional figures for pig skin assay, synthetic procedures for all compounds and results of the screening of the active compounds for PAINS and BBB penetration (PDF).

Molecular formula strings (CSV).

▪ REFERENCES

[1] WHO, https://www.who.int/news-room/detail/27-02-2017-who-publishes-list-of-bacteria-for-which-new-antibiotics-are-urgently-needed (accessed September 15, 2019)

[2] Wagner, S.; Sommer, R.; Hinsberger, S.; Lu, C.; Hartmann, R. W.; Empting, M.; Titz, A. Novel Strategies for the Treatment of Pseudomonas aeruginosa Infections. *J. Med. Chem.* **2016**, *59*, 5929–5969.

[3] Obritsch, M. D., Fish, D. N., MacLaren, R., Jung, R. Nosocomial Infections Due to Multidrug-Resistant Pseudomonas aeruginosa: Epidemiology and Treatment Options. *Pharmacotherapy* **2005**, *25*, 1353–1364.

[4] Teweldemedhin, M., Gebreyesus, H., Atsbaha, A. H., Asgedom, S. W., Saravanan, M. Bacterial Profile of Ocular Infections: a Systematic Review. *BMC Ophthalmology* **2017**, *17:212*.

[5] Lyczaka, J. B., Cannon, C. L., Piera, G. B. Establishment of Pseudomonas aeruginosa Infection: Lessons from a Versatile Opportunist. *Microbes Infect.* **2000**, *2*, 1051−1060.

[6] Hancock, R. E. W.; Speert, D. P. Antibiotic Resistance in Pseudomonas aeruginosa: Mechanisms and Impact on Treatment. *Drug Resist Updat.* **2000**, *3*, 247–255.

[7] Sordé, R.; Pahissa, A.; Rello, J. Management of Refractory Pseudomonas aeruginosa Infection in Cystic Fibrosis. *Infect Drug Resist.* **2011**, *4*, 31–41.

[8] Kim, M., Christley, S., Khodarev, N., Fleming, I., Huang, Y., Chang, E., Zaborina, O., Alverdy, J. Pseudomonas aeruginosa Wound Infection Involves Activation of Its Iron Acquisition System in Response to Fascial Contact. *J Trauma Acute Care Surg.* **2015**, *78*, 823–829.

[9] Strateva, T.; Mitov, I. Contribution of an Arsenal of Virulence Factors to Pathogenesis of Pseudomonas aeruginosa Infections. *Ann Microbiol.* **2011**, *61*, 717–732.

[10] Wretlind, B.; Pavlovskis, O. R. Pseudomonas aeruginosa Elastase and Its Role in Pseudomonas Infections. *Rev. Infect. Dis.* **1983**, 5 Suppl 5, S998–1004.

[11] Hatheway, C. L. Toxigenic Clostridia. *Clin. Microbiol. Rev.* **1990**, *3*, 66–98.

[12] Titball, R. W., Rood, J. I. 89 - Clostridium perfringens: Wound Infections. *Molecular Medical Microbiology* **2002**, *3*, 1875–1903.

[13] Granum, P. E., Lund, T. Bacillus cereus and Its Food Poisoning Toxins. *FEMS Microbiol. Lett.* **1997**, *157*, 223–228.

[14] Drobniewski, F. A. Bacillus cereus and Related Species. *Clin Microbiol Rev.* **1993**, *6*, 324–338.

[15] Matsushita, O.; Okabe, A. Clostridial Hydrolytic Enzymes Degrading Extracellular Components. *Toxicon* **2011**, *39*, 1769–1780.

[16] Harrington, D. J. Bacterial Collagenases and Collagen-degrading Enzymes and Their Potential Role in Human Disease. *Infect Immun.* **1996**, *64*, 1885–1891.

[17] Bowler, P. G., Duerden, B. I., Armstrong, D. G. Wound Microbiology and Associated Approaches to Wound Management. *Clin Microbiol Rev.* **2001**, *14*, 244–269.

[18] Guo, S., DiPietro, L. A. Factors Affecting Wound Healing. *J Dent Res.* **2010**, *89*, 219–229.

[19] Lawson, P. A., Rainey, F. A. Proposal to Restrict the Genus Clostridium Prazmowski to Clostridium butyricum and Related Species. *Int. J. Syst. Evol. Microbiol.* **2016**, *66*, 1009–1016.

[20] Zhu, J.; Cai, X.; Harris, T. L.; Gooyit, M.; Wood, M.; Lardy, M.; Janda, K. D. Disarming Pseudomonas aeruginosa Virulence Factor LasB by Leveraging a Caenorhabditis elegans Infection Model. *Chem. Biol.* **2015**, *22*, 483–491.

[21] Garner, A. L.; Struss, A. K.; Fullagar, J. L.; Agrawal, A.; Moreno, A. Y.; Cohen, S. M.; Janda, K. D. 3-Hydroxy-1-alkyl-2-methylpyridine-4(1H)-thiones: Inhibition of the Pseudomonas aeruginosa Virulence Factor LasB. *ACS Med Chem Lett.* **2012**, *3*, 668–672.

[22] Cathcart, G. R. A.; Quinn, D.; Greer, B.; Harriott, P.; Lynas, J. F.; Gilmore, B. F.; Walker, B. Novel Inhibitors of the Pseudomonas aeruginosa Virulence Factor LasB: a Potential Therapeutic Approach for the Attenuation of Virulence Mechanisms in Pseudomonal Infection. *Antimicrob. Agents Chemother.* **2011**, *55*, 2670–2678.

[23] Yiotakis, A.; Hatgiyannacou, A.; Dive, V.; Toma, F. New Thiol Inhibitors of Clostridium histolyticum Collagenase. Importance of the P3' Position. *Eur. J. Biochem.* **1988**, *172*, 761–766.

[24] Scozzafava, A., Supuran, C. T. Protease Inhibitors: Synthesis of Matrix Metalloproteinase and Bacterial Collagenase Inhibitors Incorporating 5-Amino-2-mercapto-1,3,4-thiadiazole Zinc Binding Functions. *Bioorg. Med. Chem. Lett.* **2002**, *12*, 2667–2672.

[25] Supuran, C. T.; Scozzafava, A. Protease inhibitors. Part 7: Inhibition of Clostridium histolyticum Collagenase with Sulfonylated Derivatives of L-valine Hydroxamate. *Eur. J. Pharm. Sci.* **2000**, *10*, 67–76.

[26] Clare, B. W.; Scozzafava, A.; Supuran, C. T. Protease Inhibitors: Synthesis of a Series of Bacterial Collagenase Inhibitors of the Sulfonyl Amino Acyl Hydroxamate Type. *J. Med. Chem.* **2001**, *44*, 2253–2258.

[27] Scozzafava, A., Supuran, C. T. Protease Inhibitors - Part 5. Alkyl/Arylsulfonyl- and Arylsulfonylureido-/Arylureido- Glycine Hydroxamate Inhibitors of Clostridium histolyticum Collagenase. *Eur. J. Med. Chem.* **2000**, *35*, 299–307.

[28] Flipo, M.; Charton, J.; Hocine, A.; Dassonneville, S.; Deprez, B.; Deprez-Poulain, R. Hydroxamates: Relationships between Structure and Plasma Stability. *J Med. Chem.* **2009**, *52*, 6790–6802.

[29] Kany, A. M.; Sikandar, A.; Haupenthal, J.; Yahiaoui, S.; Maurer, C. K.; Proschak, E.; Köhnke, J.; Hartmann, R. W. Binding Mode Characterization and Early in Vivo Evaluation of Fragment-Like Thiols as Inhibitors of the Virulence Factor LasB from Pseudomonas aeruginosa. *ACS Infect. Dis.* **2018**, *4*, 988–997.

[30] Schönauer, E.; Kany, A. M.; Haupenthal, J.; Hüsecken, K.; Hoppe, I. J.; Voos, K.; Yahiaoui, S.; Elsässer, B.; Ducho, C.; Brandstetter, H.; Hartmann, R. W. Discovery of a Potent Inhibitor Class with High Selectivity toward Clostridial Collagenases. J. Am. Chem. Soc. 2017, 139, 12696–12703.

[31] Martyn, D. C.; Moore, M. J.; Abell, A. D. Succinimide and Saccharin-Based Enzyme-Activated Inhibitors of Serine Proteases. *Curr Pharm Des.* **1999**, *5*, 405–415.

[32] Groutas, W. C.; Brubaker, M. J.; Chong, L. S.; Venkataraman, R.; Huang, H.; Epp, J. B.; Kuang, R.; Hoidal, J. R. Design, Synthesis and Biological Evaluation of Succinimide Derivatives as Potential Mechanism-Based Inhibitors of Human Leukocyte Elastase, Cathepsin G and Proteinase 3. *Bioorg. Med. Chem.* **1995**, *3*, 375–381.

[33] Muller, G. W.; Shire, M. Succinimide and Maleimide Cytokine Inhibitors. WO/1997/012859.

[34] https://www.drugbank.ca/drugs/DB00593; https://www.drugbank.ca/drugs/DB00832; https://www.drugbank.ca/drugs/DB05246; https://www.drugbank.ca/drugs/DB08815 (accessed September 15, 2019)

[35] Mortensen, K. T. PhD Thesis: Development of a UV-Cleavable Protecting Group for Hydroxylamines, Synthesis of a Structurally Wide Variety of Hydroxamic Acids, and Identification of Histone Deacetylase Inhibitors. Technical University of Denmark, **2017**.

[36] Nishino, N., Powers J. C. Pseudomonas aeruginosa Elastase. Development of a New Substrate, Inhibitors, and an Affinity Ligand. *J. Biol. Chem.* **1980**, *255*, 3482–3486.

[37] Baishya, J.; Wakeman, C. A. Selective Pressures During Chronic Infection Drive Microbial Competition and Cooperation. *npj Biofilms and Microbiomes* **2019**, 5:16.

[38] Woods, J.; Boegli, L.; Kirker, K. R.; Agostinho, A. M.; Durch, A.M.; deLancey Pulcini, E.; Stewart, P.S.; James, G.A. Development and Application of a Polymicrobial, In Vitro, Wound Biofilm Model. *J. Appl. Microbiol.* **2012**, *112*, 998–1006.

[39] Van Lint, P.; Libert, C. Chemokine and Cytokine Processing by Matrix Metalloproteinases and Its Effect on Leukocyte Migration and Inflammation. *J Leukoc Biol.* **2007**, *6*, 1375–1381.

[40] Sternlicht, M.D., Werb, Z. How Matrix Metalloproteinases Regulate Cell Behavior. *Annu Rev Cell Dev Biol.* **2001**, *17*, 463–516.

[41] Gooz, M. ADAM-17: The Enzyme That Does It All. *Crit Rev Biochem Mol Biol.* **2010**, *45*, 146–169.

[42] Ropero, S. Esteller, M. The Role of Histone Deacetylases (HDACs) in Human Cancer. *Mol. Oncol.* **2007**, *1*, 19–25.

[43] Chakraborty, C., Sharma, A.R., Sharma, G., Lee, S-S. Zebrafish: A Complete Animal Model to Enumerate the Nanoparticle Toxicity. *J. Nanobiotechnol.* **2016**, 14:65.

[44] MacRae, C.A., Peterson, R.T. Zebrafish as Tools for Drug Discovery. *Nat. Rev. Drug. Discov.* **2015**, *14*, 721-731.

[45] Eckhard, U., Schönauer, E., Brandstetter, H. Structural Basis for Activity Regulation and Substrate Preference of Clostridial Collagenases G, H, and T. *J. Biol. Chem.* **2013**, *288*, 20184–2019.

[46] Haupenthal, J., Baehr, C., Zeuzem, S., Piiper, A. RNAse A-Like Enzymes in Serum Inhibit the Anti-Neoplastic Activity of siRNA Targeting Polo-Like Kinase 1. *Int. J. Cancer* **2007**, *121*, 206−210.

[47] Maes, J.; Verlooy, L.; Buenafe, O. E., de Witte, P. A. M., Esguerra, C. V., Crawford, A. D. Evaluation of 14 Organic Solvents and Carriers for Screening Applications in Zebrafish Embryos and Larvae. *PLoS One* **2012**, *7*, e43850.

[48] Elgaher, W., Fruth, M., Groh, M., Haupenthal, J., Hartmann, R. W. Expanding the Scaffold for Bacterial RNA Polymerase Inhibitors: Design, Synthesis and Structure–Activity Relationships of Ureido-Heterocyclic-Carboxylic Acids. *RSC Adv.* **2014**, *4*, 2177–2194.

TABLE OF CONTENTS

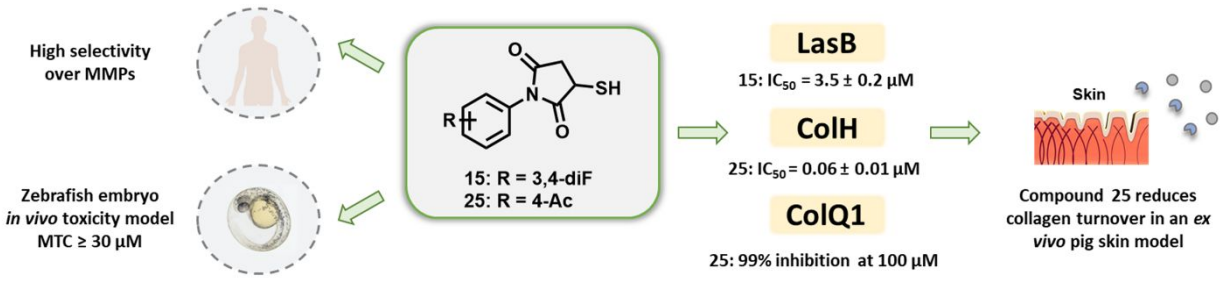

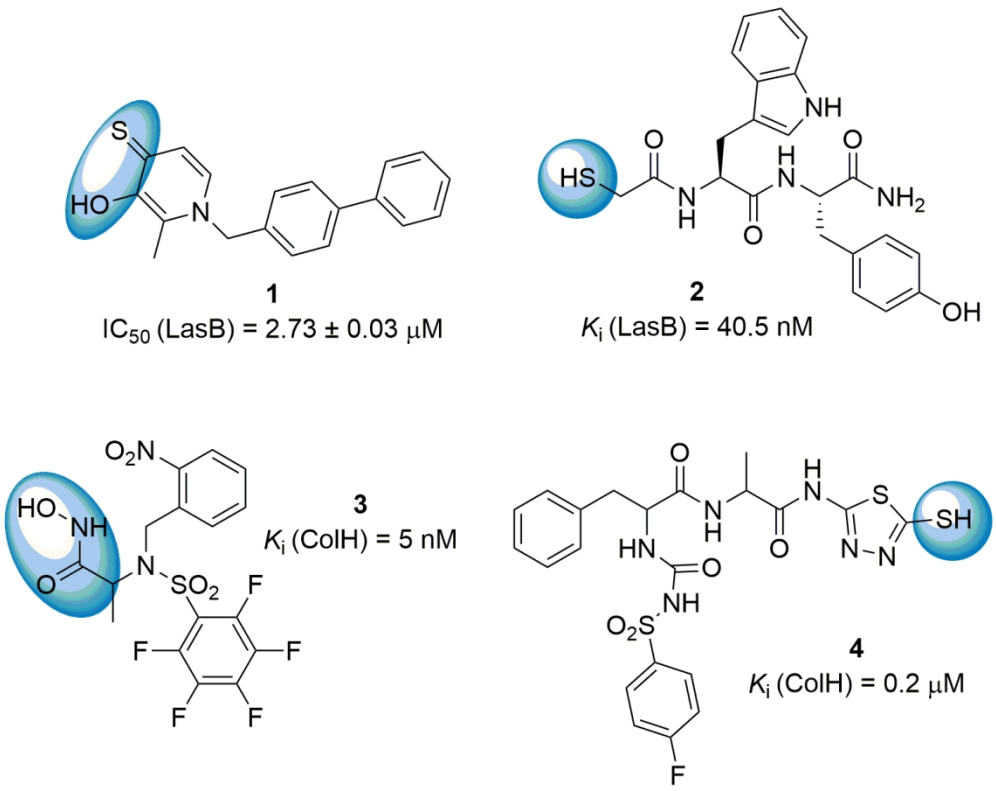

Figure 1. Structural motifs of some LasB and ColH inhibitors described in the literature (Zn-binding groups are highlighted in blue).

132x104mm (300 x 300 DPI)

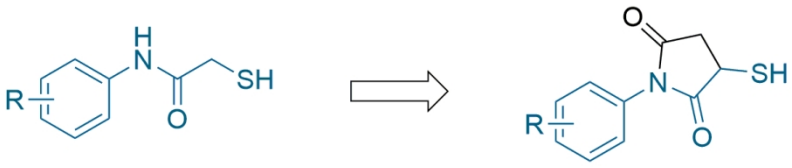

N-aryl mercaptoacetamides 3-mercapto-*N*-arylsuccinimides

5: R= 3,4-di-Cl **(IC_{50} (LasB) = 6.6 ± 0.3 µM)**
6: R= 4-Ac **(IC_{50} (ColH) = 0.017 ± 0.002 µM)**

Figure 2. Our previous results and the design of new inhibitors.

128x43mm (300 x 300 DPI)

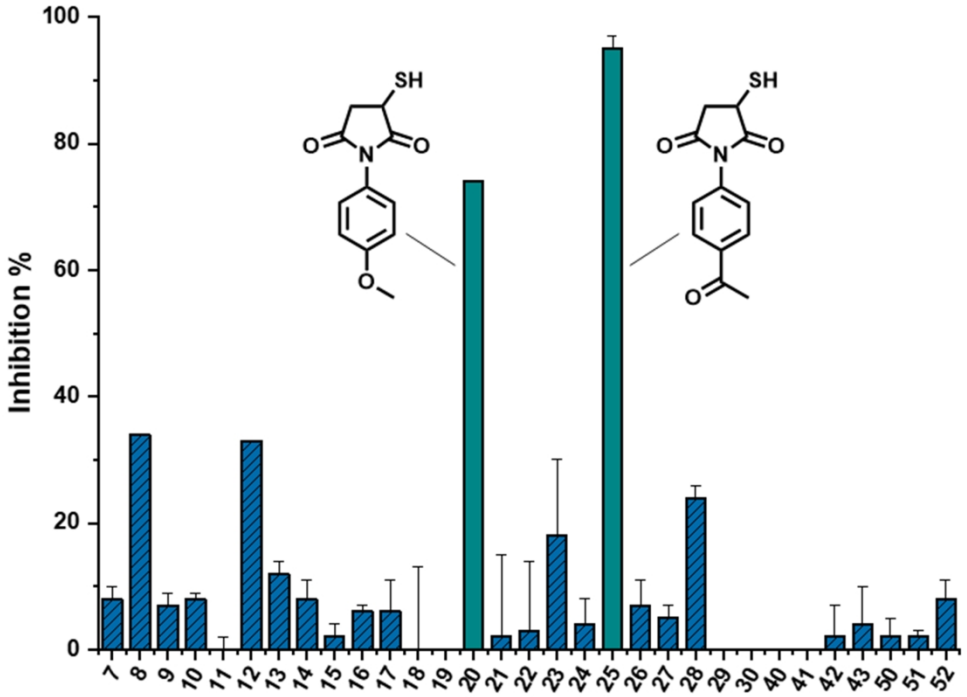

Figure 3. Inhibition of the peptidolytic activity of ColH-PD in the presence of 1 μM of the respective compound in a FRET-based assay: para-acetyl substituent in compound 25 proved to be the most beneficial substitution for the activity. Data are presented as means and SD of three independent experiments.

250x192mm (300 x 300 DPI)

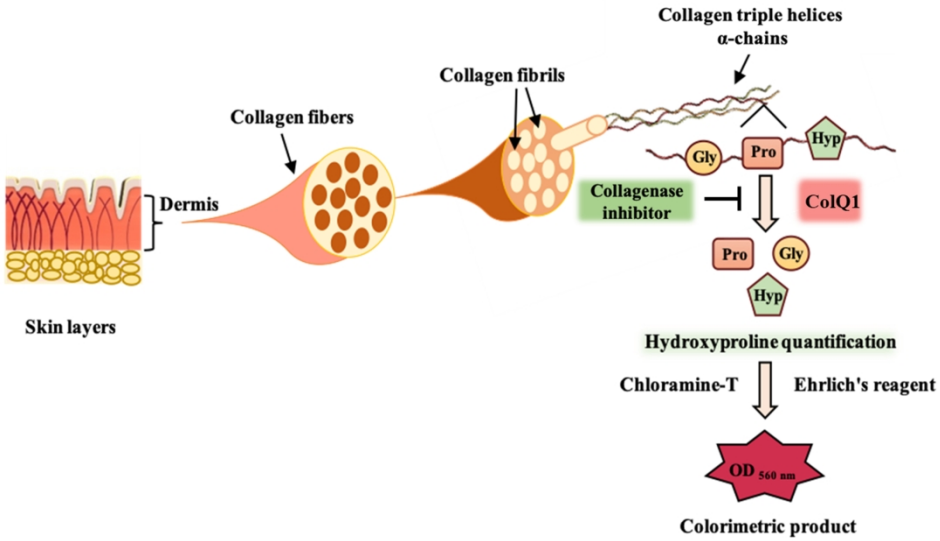

Figure 4. Representation of the pig skin model: the composition of the skin, the dermal layer and the amino acids of collagen are illustrated. The concept of the hydroxyproline quantification assay is explained by mixing chloramine-T and Ehrlich's reagent to obtain a product that can be detected with a spectrophotometer.

338x190mm (300 x 300 DPI)

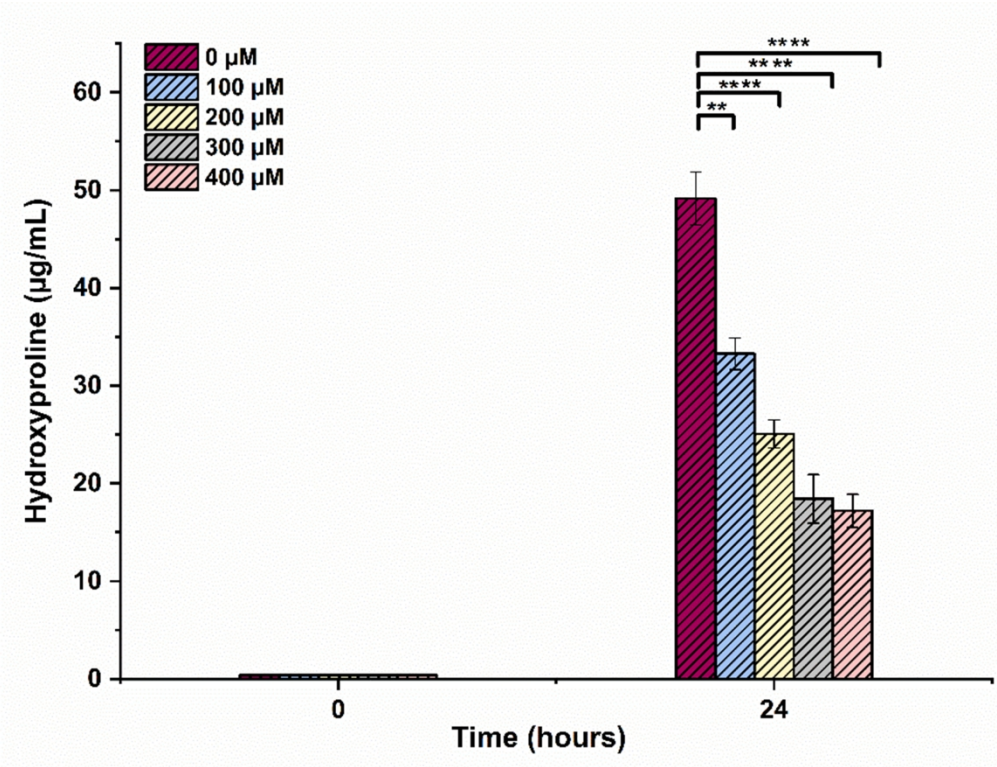

Figure 5. The amount of hydroxyproline at different concentrations of 25. Data shown represent the means ± SD from three independent measurements. One-way ANOVA followed by Tukey's HSD test (** = $p < 0.01$, **** = $p < 0.0001$).

246x188mm (300 x 300 DPI)

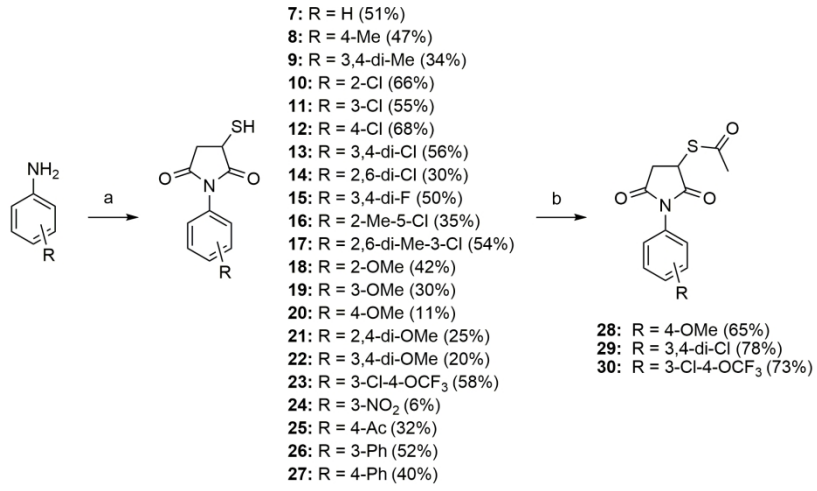

Scheme 1. Synthesis of novel free thiol succinimides and thioacetate derivatives

201x107mm (300 x 300 DPI)

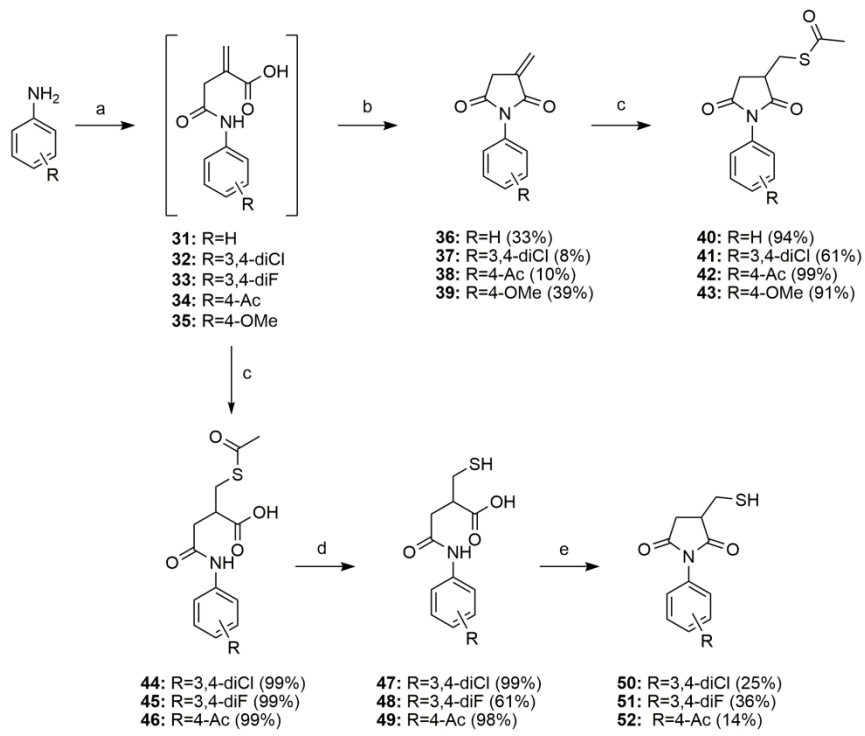

Reagents and conditions: (a) itaconic anhydride, $CHCl_3$, 2 h, r.t.; (b) Ac_2O, NaOAc, 1–2 h, 100 °C; (c) AcSH, Et_3N, DME or THF, r.t.; (d) 2 M NaOH, MeOH, 2 h, r.t.; (e) 120 °C, Ar, neat, overnight

Scheme 2. Synthesis of N-aryl-3-mercaptomethylsuccinimides and their thioacetyl analogs

201x161mm (300 x 300 DPI)

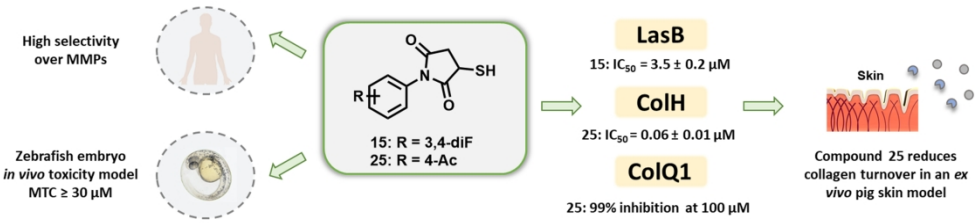

209x54mm (300 x 300 DPI)